2018-04-01

Simulation of the Inertia Friction Welding Process Using a Subscale Specimen and a Friction Stir Welder

Ty Samual Dansie
Brigham Young University

Simulation of the Inertia Friction Welding Process

Using a Sub-Scale Specimen and

a Friction Stir Welder

Ty Samual Dansie

A thesis submitted to the faculty of
Brigham Young University
in partial fulfillment of the requirements for the degree of

Master of Science

Carl D. Sorensen, Chair
Tracy W. Nelson
Michael P. Miles

Department of Mechanical Engineering

Brigham Young University

ABSTRACT

Simulation of the Inertia Friction Welding Process
Using a Sub-Scale Specimen and
a Friction Stir Welder

Ty Samual Dansie
Department of Mechanical Engineering, BYU
Master of Science

This study develops a method to simulate a full-scale inertia friction weld with a sub-scale specimen and modifies a direct drive friction stir welder to perform the welding process. A torque meter is fabricated for the FSW machine to measure weld torque. Machine controls are modified to enable a force control during the IFW process. An equation is created to measure weld upset due to deflection of the FSW machine. Data obtained from a full-scale inertia friction weld are altered to account for the geometrical differences between the sub-scale and full-scale specimens. The IFW are simulated with the sub-scale specimen while controlling spindle RPM and matching weld power or weld RPM. The force used to perform friction welding is scaled to different values accounting for specimen size to determine the effects on output parameters including: HAZ, upset, RPM, torque, power and energy of the weld. Increasing force has positive effects to upset, torque, power and energy of the welds, while reducing the size of the HAZ.

Keywords: rotary friction welding, inertia friction welding, direct drive friction welding, welding, inconel-718, simulating, flywheel, energy, nickel based superalloy, subscale modelling

ACKNOWLEDGMENTS

I would like to thank my committee for their expert advice, valued time and their continual direction of my research; I would not be able to accomplish all that I have without them. I would like to thank my colleagues for their insight on complicated problems and continuous support. I would also like to thank my wife for her continued motivation and aid in staying on task during this research.

Financial support for this work was provided by General Electric and the grant for Friction Welding research.

TABLE OF CONTENTS

LIST OF TABLES

LIST OF FIGURES

NOMENCLATURE

FRW	Rotary Friction Welding
DDFW	Direct Drive Friction Welding
IFW	Inertia Friction Welding
FSW	Friction Stir Welding
SIFW	Simulated Inertia Friction Welding
FS	Full Scale Specimen
SS	Sub Scale Specimen
ω	Spindle rotational velocity
I	Flywheel Inertia
E	Energy
F	Force
dt	change in time
P	Power
τ	Torque
kN	kilonewtons
mm	millimeter
RPM	Revolutions per minute
kW	kilowatts
W	watts
Nm	Newton-meters
J	Joules
r	Radius
t	Thickness
A	Cross Sectional Area
Z	Machine Position
k	machine compliance
fr	feedrate
HAZ	heat affected zone
P_{cmd}	Power commanded
P_{exp}	Power expected
F_{cmd}	Force commanded
F_{exp}	Force expected
RPM_{cmd}	RPM commanded
RPM_{exp}	RPM expected

CHAPTER 1. INTRODUCTION

1.1 Background of Friction Welding

Rotary friction Welding (FRW) is a solid state joining process in which the heat for welding is produced by the friction induced through the relative motion of two interfaces being joined. The coalescence of materials is obtained through the combined effects of the pressure and relative motion of the two work pieces, heating the joint interface, and inducing plastic deformation of the material, as shown in Figure 1.1 [1] [2]. Heat generation is due to the conversion of the kinetic energy of the moving objects into thermal or mechanical energy [3]. After the material has been softened the specimens are forged together to produce the weld. This method of welding is advantageous over other methods because it requires less power input per weld in mass production and allows the binding of various dissimilar metals [4]. Despite FRW's frequent use, the joining phenomena during the friction process such as joining behaviour, friction, process torque, temperature changes at the weld interface, and transitional changes in material of the weld interface are still not completely understood [5] [6].

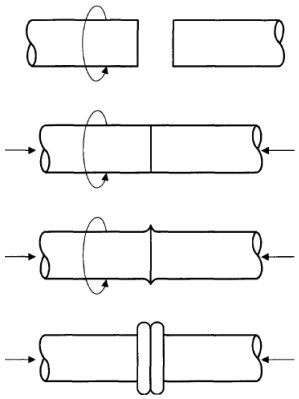

Figure 1.1: Rotary friction welding process [13].

1.2 Friction Welding

FRW has two primary methods, inertial friction welding (IFW) and direct drive friction welding (DDFW). Both processes can produce excellent solid state bonds. There are subtle differences or advantages of one process over the other. DDFW is primarily used for smaller specimens while IFW is often used for larger specimens due to the torques involved. However, these advantages are not universal but depend upon the application (size, material, combination, and geometry consideration) [7] [9].

1.2.1 Direct Drive Friction Welding

In DDFW a lathe-like machine rotates one piece while the other piece is pressed against the rotating piece with a certain force to produce the weld. DDFW uses a spindle connected directly to a motor. This spindle maintains a specified constant RPM while performing the weld [8]. While the spindle is rotating a friction force is applied. When the weld has finished the friction phase the spindle is stopped and a forging force is applied to complete the weld [1]. This forging force is held for a predetermined time. Welding inputs are the RPM of the spindle, time of the weld, friction force, and forging force [3]. Representative profiles of the force, speed, and upset can be seen in Figure 1.2

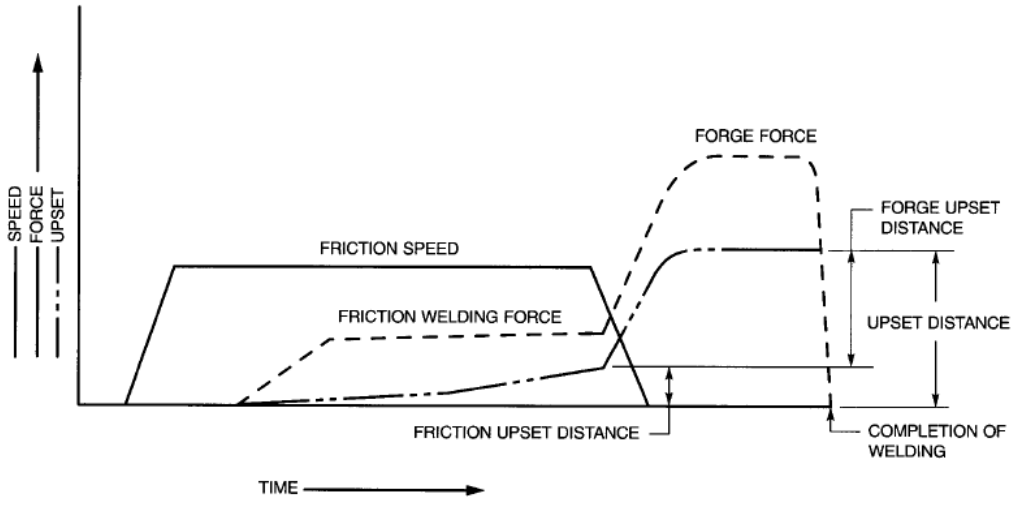

Figure 1.2: Direct drive friction welding parameters including force, RPM, and upset versus time. The weld commences when the welding force is applied [13].

1.2.2 Inertial Friction Welding

In IFW a flywheel is attached to one piece and raised to a specified speed, after which the other piece is pushed against the rotating piece with a certain force to produce the weld. Flywheel inertia and initial RPM of the flywheel determine the energy available for the weld. Inertial energy from the spinning flywheel is converted to heat at the weld interface [9] [2]. The upset of the weld is determined by the friction force and subsequent forging force applied by the non-rotating specimen. The inputs of IFW are friction force, forging force, and initial friction speed and the output is the upset or displacement of a IFW and the RPM rundown curve and can be seen in Figure 1.3.

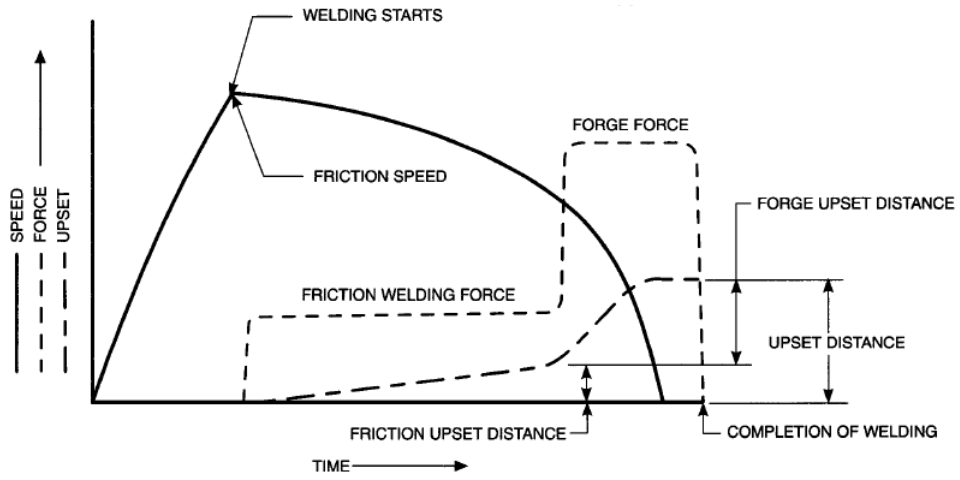

Figure 1.3: Inertia friction welding parameters including force, RPM, and upset versus time. The weld commences when the welding force is applied [13].

1.3 Friction Welding Research

Due to high costs of IFW research with full-scale specimens and available machinery, research is needed to be performed with sub-scale specimens and with the use of a FSW machine versus an industrial friction welder [2]. This research modifies data from a full-scale IFW to produce welds with sub-scale specimens on the modified FSW machine. This sub-scale simulation of the full-scale specimen will be termed as the simulation of inertia friction welding (SIFW). The

measurements that have been obtained by the full-scale IFW process include the RPM, inertia flywheel size, upset, time, the force of the weld, and the width of the HAZ. The IFW measurements will be modified to account for the changes in specimen size. The modifications to data will provide the input parameters to use when simulating a full-scale IFW with a sub-scale specimen on a modified FSW machine.

1.4 Thesis Introduction

This thesis covers the modifications to data and machinery and analyzes welds performed with changes in the SIFW process. Chapter one discusses the machine controls modifications and their impact on machine accuracy. Chapter 2 presents the machine modifications to control the RPM and the force of the weld. Chapter 4 considers weld data manipulation and accounting for changes in weld size, taking into account the area, thickness and radius of the specimens are then discussed. Welds are performed and analyzed accounting for varying forces, RPMs, and power to change the output parameters of the weld. A conclusion is then derived to determine the preferred inputs of weld control.

CHAPTER 2. SUB-SCALE SPECIMEN CORRECTIONS

Adjustments to welding parameters should be considered when IFW specimens with identical material and changes in geometry. The full-scale IFW and the sub-scale simulated inertia friction weld (SIFW) have inherent differences when it comes to the geometry, and the data from the full-scale IFW was modified to account for these differences. The differences between the full-scale and the sub-scale specimens are significant and the best way to scale the parameters between welds had not been researched and was a large part of this research. The full-scale IFW weld is 2.313 inches in diameter and has a wall thickness of 0.15 inches. The sub-scale simulated inertia friction weld (SIFW) sample is 1 inch in diameter and has a thickness of 0.1 inches. Certain assumption about the inputs and outputs of the process were made to produce scaled values for the SIFW and are described in the following sections. These assumptions make it possible to simulate an FS IFW with a sub-scale specimen.

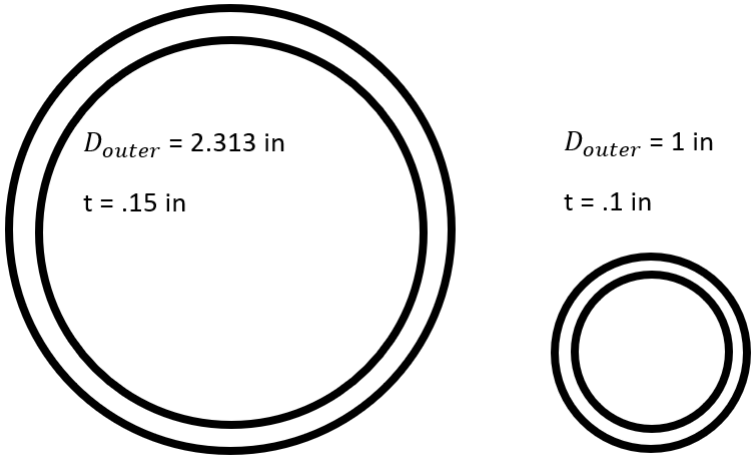

Figure 2.1: Full-scale and sub-scale specimen diameter and thickness.

The input and output parameters of interest to simulate are RPM, torque, power, force, upset, and the HAZ. The size of the specimen directly affects the RPM, torque, power, and force

of the weld and the ability to match these parameters will be based upon the radius and/or the thickness of the material. A theory is developed to determine the ratio at which the RPM, torque, power and force of the weld will scale with changes in specimen size. The scaling relation between the HAZ and the upset are theorized to scale by a 1:1 ratio with changes in specimen size.

2.1 Adjusting Spindle RPM

The RPM of the spindle is one parameter that was modified to simulate the IFW process. The RPM and the radius of the specimen produce the relative motion required for FRW, which produces the heating of the joint interface and induces plastic deformation [1] [2]. This research attempts to match the relative velocity to produce equal heating of the joint interface. To match the relative velocity the RPM of the full-scale IFW (RPM_{FS}) was scaled to the sub-scale SIFW (RPM_{SS}) as seen Equation 2.1.

$$\frac{RPM_{SS}}{RPM_{FS}} = \frac{r_{FS}}{r_{SS}} \tag{2.1}$$

The scaled value of RPM for the SIFW will be the full-scale IFW RPM multiplied by a factor of 2.313.

2.2 Welding Torque

The expected scaled value of the torque during the weld was assumed to be related to the shear stress acting at the welding interface. During the welding process a shear stress (τ) is present as the rotating specimen rotates. The welding torque (T) is due to the shear force (F) acting at a certain distant from center line (r).

$$T = F \cdot r \tag{2.2}$$

This force is a function of the shear stress acting over an infinitesimal area (dA) of the specimen

$$F = \tau dA \tag{2.3}$$

integrating this force over an entire rotation of the specimen gave us:

$$F = \tau r t 2\pi \tag{2.4}$$

where (t) is the thickness of the specimen. This produced an equation for the torque of the weld combining Equations 2.2 and 2.4.

$$T_{SS} = \tau_{SS} t_{SS} r_{SS}^2 2\pi \tag{2.5}$$

$$T_{FS} = \tau_{FS} t_{FS} r_{FS}^2 2\pi \tag{2.6}$$

If shear stress between the two components are assumed to be equal then ratio of the sub-scale torque and the full-scale torque is seen as:

$$\frac{T_{SS}}{T_{FS}} = \frac{t_{SS} r_{SS}^2}{t_{FS} r_{FS}^2} \tag{2.7}$$

producing a factor of 0.125. Thus the scaled sub-scale SIFW torque is the full-scale IFW multiplied by the factor of 0.125.

2.3 Power

To account for the reduced power input required for the SS SIFW the purpose and source of power is considered. The purpose of matching the power input is to match the heat input which. The heat input can be derived as the Equation 2.8 [15].

$$Q = \omega \tau \tag{2.8}$$

Taking into account torque and RPM, the power factor can be calculated by the product of the rpm and the torque factors. The power factor was calculated combining Equations 2.1 and 2.7.

$$\frac{P_{SS}}{P_{FS}} = \frac{t_{SS} r_{SS}}{t_{FS} r_{FS}} \tag{2.9}$$

The sub-scale SIFW was scaled to be equal to the full-scale IFW multiplied by the power factor which produced a factor of 0.2882.

2.4 Energy Density

To account for the geometrical volume difference due to the upset and area a final factor of energy density into the weld was looked at. Looking at the energy density can help determine the amount of energy placed into the weld with respect to volume and compare the sub-scale sample to the full-scale sample. The energy per unit volume could be seen as Equation 2.10

$$Energy_d = \frac{Energy}{Az} \tag{2.10}$$

where A is the area and z is the upset.

$$Energy_d = \frac{Energy}{2\pi rtz} \tag{2.11}$$

To calculate the factor considering area and upset

CHAPTER 3. FSW MACHINE MODIFICATIONS

The FSW machine required two types of changes. The first changes were made to accurately measure weld torque and weld upset. The second changes were to enable the FSW machine to control inputs, such as power or rpm and force, to simulate an IFW.

3.1 Measurement Modifications

To improve the measurement capability of the machine, a torque meter was developed and installed and the machine compliance was calibrated.

3.1.1 Torque Meter

When the spindle speed is not constant, the spindle torque as measured by the motor controller is incorrect. Testing of the spindle in the air showed that measured motor torque did not equal weld torque. Figure 3.1 depicts the RPM and indicated spindle torque of the testing in air over a given time with changes in RPM. When the spindle speed was decreased a braking torque

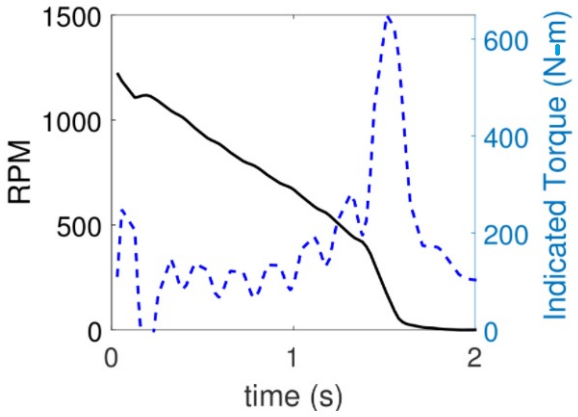

Figure 3.1: Spindle RPM and torque versus time for an air test.

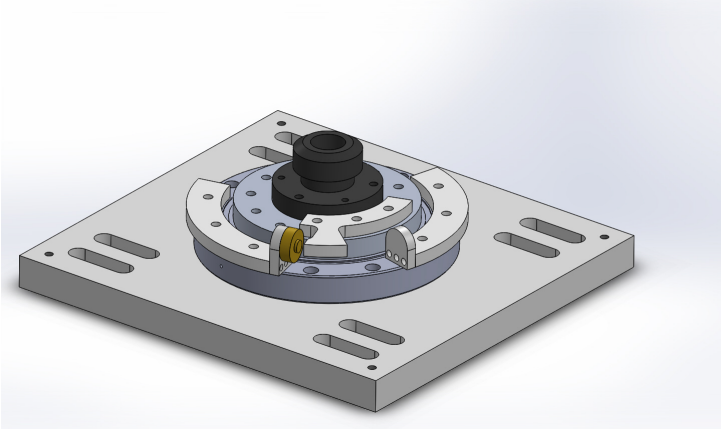

Figure 3.2: Spindle RPM and torque versus time for an air test.

was applied by the motor to the spindle. The FSW machine machine read the torque of the spindle motor which does not represent the torque of the weld, which would be zero in this test.

A torque meter was designed, fabricated, and installed on the machine in order to measure the welding torque and can be seen in Figure 3.2 and a larger image can be seen in Appendix B. A load cell was placed 4.4 inches away from the center of the specimen and a lever arm was used to push a load cell. The load cell made it possible to measure the torque at the weld interface. The torque meter also held the lower sample stationary against the bed of the machine while the upper portion of the machine rotated the upper specimen and pushed with a given force.

3.1.2 Machine Mechanical Compliance Calibration

To measure the upset of the weld, the mechanical compliance of the machine was accounted for. The measured position of the machine did not match the weld upset when a force is present, due to mechanical compliance of the machine. To account for the mechanical compliance, testing was done to accurately measure the position of the machine or weld upset while accounting for the affect that force had on the measured position.

Testing the mechanical compliance consisted of placing a tool in the head against the bed of the machine, zeroing the position, varying the force, and observing head position. During testing the position of the machine was read at zero newtons of force. The force was then increased incrementally and position measurements were taken, while the actual position of the machine did not change, measured position did. The mechanical compliance was determined, which allowed

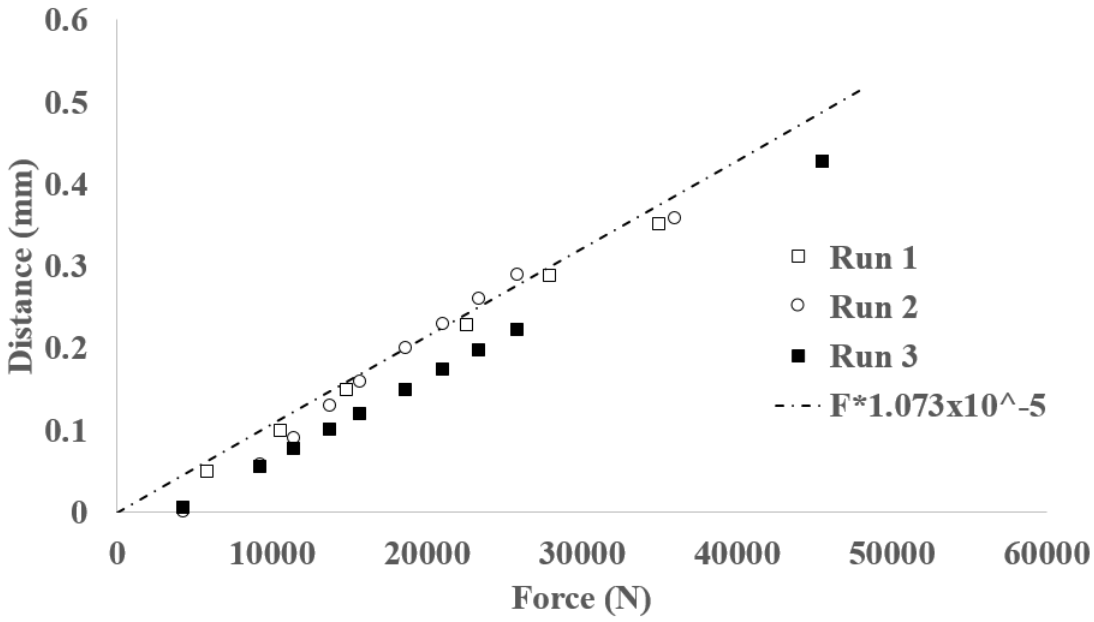

Figure 3.3: Deflection of the machine readings while increasing and decreasing force.

Table 3.1: Machine deflection testing results.

Run	**Compliance (mm/N) x 10^{-5}**
1	.9699
2	1.006
3	1.378
Averaged	1.073

the actual position of the weld or the upset of the piece to be determined. Figure 3.3 shows the results from the testing of the mechanical compliance. This testing displayed the difference between measured and actual position that can occur while welding a piece with changes in the applied force.

The experiments performed determined the amount of deflection that occurred for a given force. The amount of deflection per unit force from the three experiments can be seen in Table 3.1 and the deflections of .9699, 1.006, and 1.378 were averaged to create 1.073 which is used in Equation 3.1 to determine the weld upset.

$$Upset = Z - F * 1.073 \cdot 10^{-5} \tag{3.1}$$

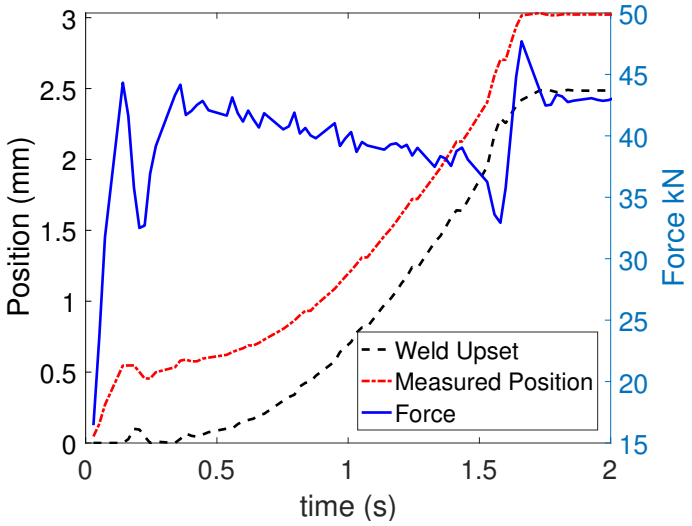

Figure 3.4: A comparison of the machine measured position and weld upset (actual position) taking into account force versus time.

Equation 3.1 takes the current force (F) of the machine and the measured position (Z) of the piece and converts it to the upset of the weld. The upset calculated from Equation 3.1 is used in the remainder of the paper as the position of the piece. The calculated upset is plotted versus time and compared to the measured position in Figure 3.4.

3.2 FSW Machine Control Alterations

To enable the FSW machine to produce SIFW, machine time delays were accounted for and spindle speed controls and machine position controls were modified.

3.2.1 RPM Time Delay Correction

A time delay exist between the time that the RPM is commanded to the time the spindle attains the commanded RPM. To determine the size and location of the time delay, a test was designed to measure the time delay. The RPM was commanded from MATLAB as seen in Figure 3.5. A series of RPM jumps were programmed to account for the differences in commanded and desired RPM. This testing commanded RPM from MATLAB to determine the location of delay.

During the testing the commanded RPM of the spindle did not match the desired RPM. It can be seen in Figure 3.6 that the primary source of the time delay was the spindle controller. The

time delay existed before the actual RPM reached the desired RPM due to the spindle controller accounting for the physics of the motor. Figure 3.7 shows that as the change in RPM got greater the time to reach the RPM was increased. The time delay of .20 seconds was used to enable the commanded RPM to produce an actual RPM that matched desired RPM.

3.2.2 Spindle Control Testing

Two methods of spindle control are used to simulate the IFW process. One method, power match, consisted of matching spindle power by controlling spindle RPM, which read the torque of the weld and commanded an RPM of the spindle to match the desired power into the weld using Equation 4.6.

$$RPM = \frac{P_{desired}}{T} \tag{3.2}$$

The desired power was pre-programmed and was a fraction of the FS IFW. The second method matched a scaled RPM, programmed the spindle to follow a factor of the FS IFW rundown curve.

While matching weld power, the spindle RPM was initialized at 1500 and 1000 to determine the machine's ability to control spindle RPM with drastic changes in RPM while matching weld power without failing. While controlling the spindle RPM with an initial RPM of 1500, spindle control failed when the RPM was commanded to change. As evident in Figure 3.8a, the actual RPM representing the spindle RPM begins a coast down instead of following the commanded RPM in blue. Spindle control was lost due to a circuit protection designed to prevent overheating the transistors in the circuitry. The default of the FSW machine programming is to protect circuitry, which releases the spindle and its affect on spindle RPM can be seen in Figure 3.8a. Subsequent power controlled welds were ran with an initial speed of 1000 RPM as seen in Figure 3.8b and at 1000 RPM the FSW machine did not lose control. Initializing the RPM at 1000 was chosen because it preserved control of the spindle throughout the weld.

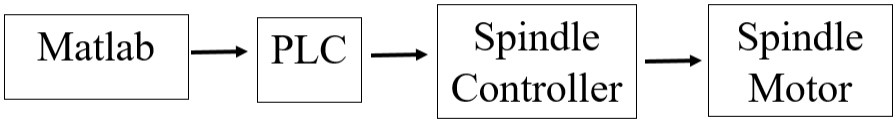

Figure 3.5: Commanded spindle RPM logic flow.

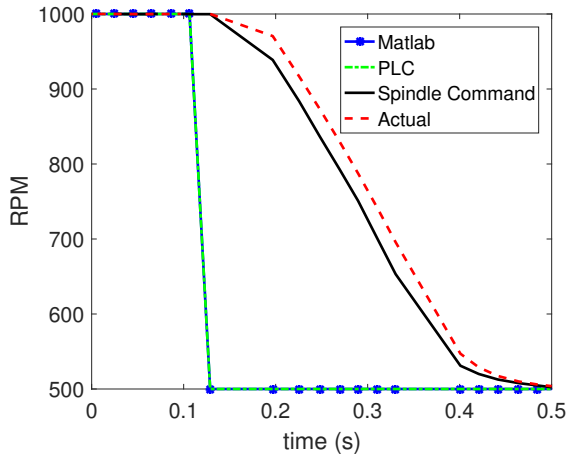

Figure 3.6: RPM command values from MATLAB, the PLC, the spindle controller and the actual spindle RPM with a change from 1000 to 500 RPM.

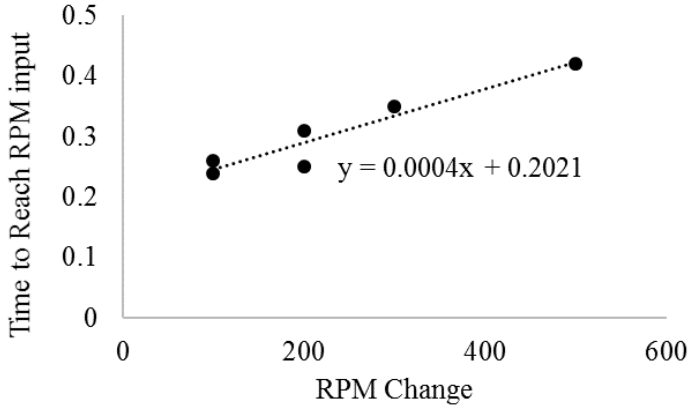

Figure 3.7: Time delay of spindle with changes in RPM.

3.2.3 Force Control

To control the force of the FSW machine, modifications were performed on the feed methods of the machine. The default feed method for the FSW machine is position controlled, but the FSW controller has an algorithm that can control force based upon the the pre-programmed machine compliance (k) setting and maximum feedrate. Modifying the k and the maximum feedrate increased the accuracy of the FSW machine to maintain a certain welding force. A welding force was then able to be input versus a feedrate or position. Establishing force control for the FSW machine is vital for a simulation of an IFW.

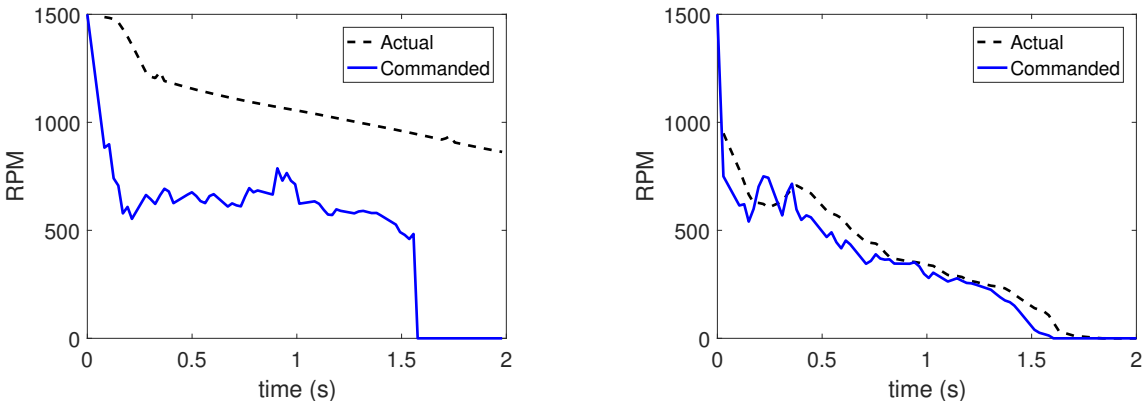

Figure 3.8: (a) RPM versus time of a power matched weld with an initial RPM of 1500. (b) RPM versus time of a power matched weld with an initial RPM of 1000.

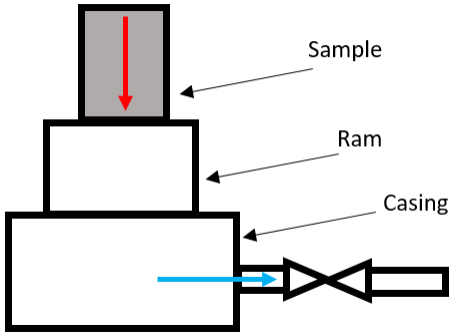

Figure 3.9: Assembly used to test and establish values for force control.

The k and maximum feedrate of the machine were tested using a bottle jack and a simplified system drawing can be seen in Figure 3.9. The sample was placed into the upper fixture of the machine and pushed against the ram of the bottle jack. The adjustments of the valve and the amount of force determined the rate at which ram would descend into the casing and allow the ram to move downward. This testing produced a force that was proportional to the FSW machine feedrate. During programmed machine compliance testing the valve was open slightly and the head of the machine was given a force of 35,000 or 30,000 Newtons and maximum feedrate was set to 5 mm/s. During maximum feedrate testing the valve was closed and the machine was tested to determine the a feedrate necessary to reach the force in 0.4 seconds.

3.2.3.1 Programmed Compliance Value

The programmed compliance value (k) determines the amount of travel necessary to reach the target position. The higher the k-value the more the head is designed to move to reach a given force.

The k of the machine was tested to determine a value that would attain the force commanded in minimal amount of time while accounting for overshoot and the error at steady state. Testing performed with a feedrate of 5 mm/s showed that changes in the programmed machine compliance (k) affected the time to attain programmed force as seen in Figure 3.10b. Also noticed in Figure 3.10b is the overshoot with a k value of .04. A steady state error is also observed with different values of k. The programmed force was 30 kN but the FSW machine only reached a consisten force of 29 kN, the 1 kN difference is considered the steady state error. Figure 3.11 takes a closer look at the steady state error with changes in k, as k was increased from 0.008 to 0.032 the steady state error was observed to decline. When k was increased to a value of 0.040, the steady state error increased. It was determined that a k value of 0.032 produced the least steady state error, no overshoot and would be used to for force control in all subsequent welds.

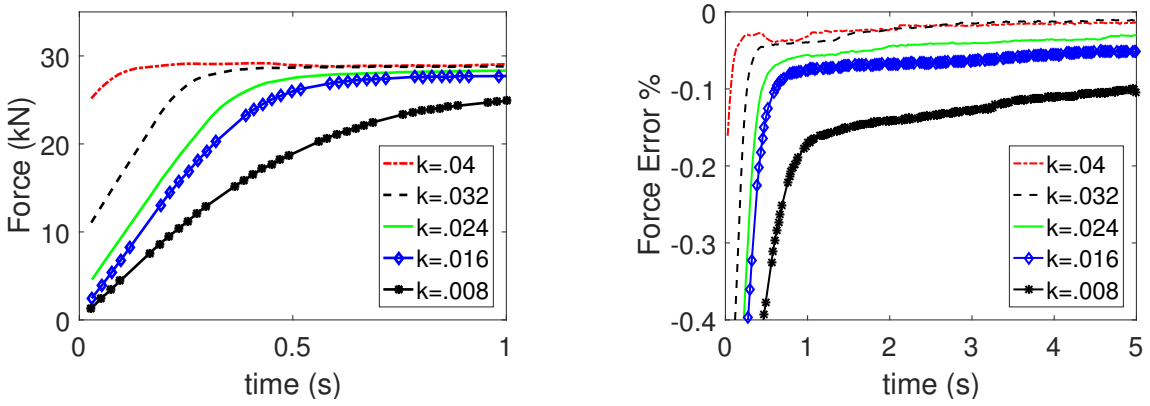

(a) (b)

Figure 3.10: (a) Force versus time with varying k values. (b) Error versus time with varying k values.

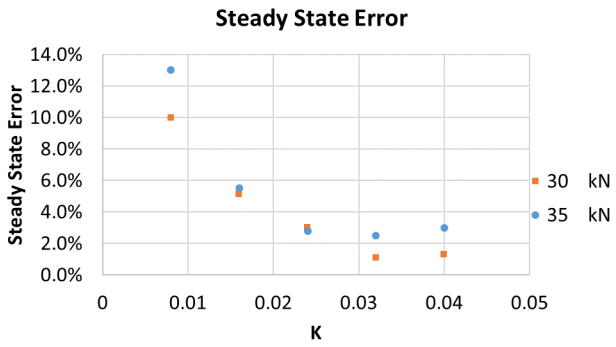

Figure 3.11: Programmed machine compliance versus Force steady state error at 35 and 30 kN.

3.2.3.2 Feedrate

Maximum feed-rates were then tested, with the k obtained from testing, and the feedrate was adjusted to allow force control of the FSW machine to reach the programmed 62 kN force in approximately 0.5 seconds. The controller works by plunging the work piece at the programmed feed rate; then, as the force approaches the programmed force, the feed rate decreases as a linear function of the maximum feedrate.

Using the k previously found in the k value testing, experiments altering the feedrate showed that feedrate drastically affected the rate at which the machine could reach the desired force. Figure 3.12 shows that as the feedrate was increased, the time to reach the target force of 62000 Newtons was decreased. The feedrate chosen to be used in the simulation of the IFW process was 7 mm/s or 420 mm/min.

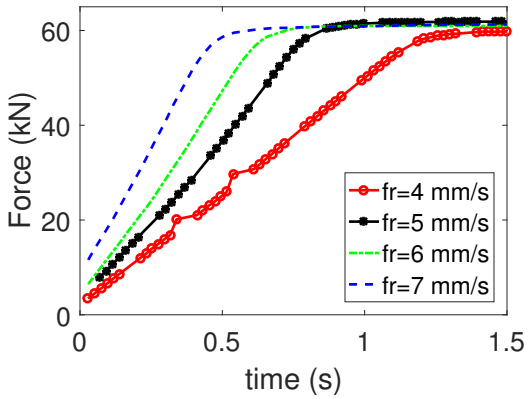

Figure 3.12: Time to reach desired force with k=0.032 and changes in feedrate (fr).

3.3 Conclusion

The modifications and testing performed on the FSW machine allowed the FSW machine to control and measure welding variables accurately. The weld measurements of position now account for the mechanical compliance of the machine, to accurately measure weld upset. The torque of the weld is now measured to enable accurate control over weld power. Initially the FSW machine was programmed to control the position of the machine and maintained a constant spindle RPM. The modifications to the FSW machine allowed control of changing spindle RPM and spindle power matching with the use of a torque meter. In addition, the FSW machine now has the ability to control the force of the weld with a programmed machine compliance value of 0.032 and a maximum feedrate of 7 mm/s.

CHAPTER 4. SIMULATING INERTIA FRICTION WELDING METHODS AND RESULTS

Using the IFW data obtained from a full-scale Inconel specimen different experiments were designed to determine suitable inputs for a sub-scale specimen to produce expected scaled outputs. A method to control the spindle both power and rpm mode were determined. Forces were varied to obtain different results and to determine a method that could properly simulate a FS IFW with a sub-scale specimen.

4.1 Material

Welding materials of the two specimens were Inconel-718 and the composition and makeup can be seen in Table 4.1. Prior to welding, the surfaces of the sub-scale specimens were cleaned with acetone to remove debris or contaminants from the welding surface.

Table 4.1: Inconel 718 chemical composition.

Element	**C**	**Mn**	**Si**	**Cr**	**Ni**	**Mb**	**Nb**	**Ti**	**Al**	**Fe**
Wt. %	.1	.2	.3	18.2	52.9	3	5	.8	.5	19.0

4.2 Inertia Friction Welding Data and Conversion

The IFW data consisted of force, upset, spindle velocity (ω), time and the inertia of the flywheel (I), other parameters were calculated from these parameters. The force, position and spindle velocity can be seen in Figures 4.1 - 4.3. The energy (E) of the flywheel was calculated using Equation 4.1

$$E_o = \frac{1}{2}\omega_o^2 \cdot I \tag{4.1}$$

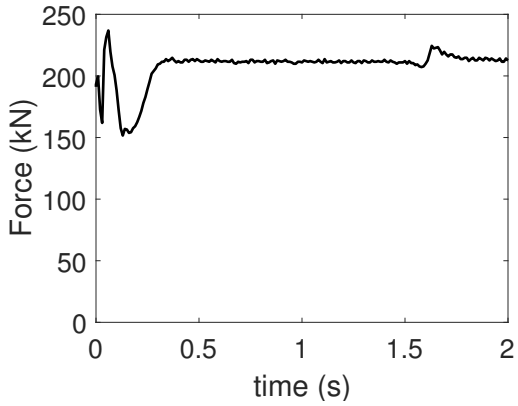

Figure 4.1: Force versus time data of the IFW of Inconel-718 weld.

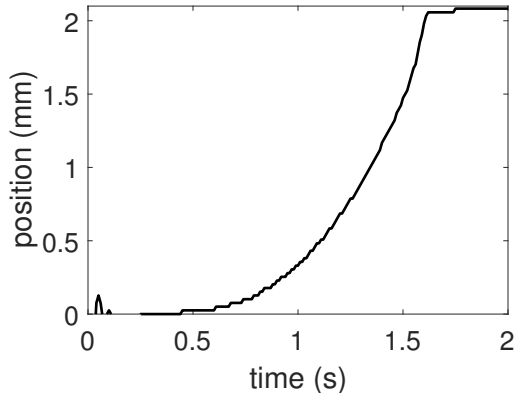

Figure 4.2: Position versus time data of the IFW of Inconel-718 weld.

Weld power (P) was calculated as the change in energy of the flywheel with the change in time (dt) as seen in Equation 4.2

$$P = \frac{E_i - E_{i-1}}{dt} \tag{4.2}$$

Taking the derivative of Equation 4.1 gave us:

$$\frac{dE}{dt} = I\omega\frac{d\omega}{dt} \tag{4.3}$$

and when the power is also equal to the product of the weld torque (τ) and the spindle velocity (ω).

$$\frac{dE}{dt} = \tau\omega \tag{4.4}$$

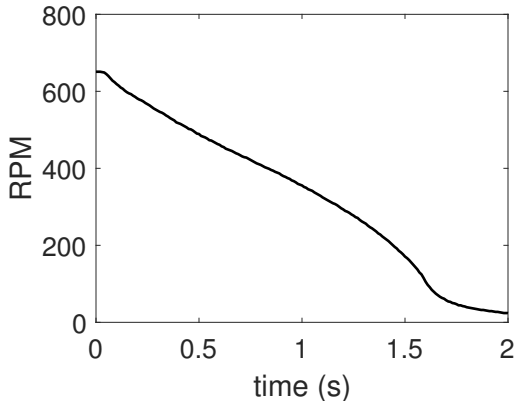

Figure 4.3: Spindle RPM versus time data of the IFW of Inconel-718 weld.

Combining Equation 4.3 and Equation 4.4 shows that torque is equal to the product of flywheel inertia and the change in the velocity of the spindle.

$$\tau = I\frac{d\omega}{dt} \tag{4.5}$$

Torque is then set equal to the power of the weld divided by the spindle velocity as seen in Equation 4.6

$$\tau = \frac{P}{\omega} \tag{4.6}$$

To minimize any noise in the calculated data, a total variation minimization filter was applied to the FS IFW RPM data. The filtering of the RPM data provided a more stable reading for the FS IFW RPM and the calculations of the FS IFW power, FS IFW torque and FS IFW energy data.

4.2.1 Filtered and Calculated IFW Data

The original IFW data was obtained and with the use of a Total Variation Minimization (TV) filter [14], noise was minimized and output parameters were calculated. The TV filter was used to filter the RPM readings to minimize noise obtained from the measuring equipment. Figure 4.4a shows the RPM measured with the RPM obtained from the TV filter. The change in RPM ($\frac{dw}{dt}$) was also placed through the filter.

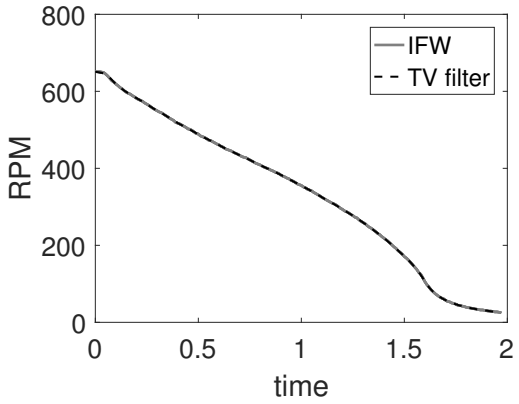

(a)

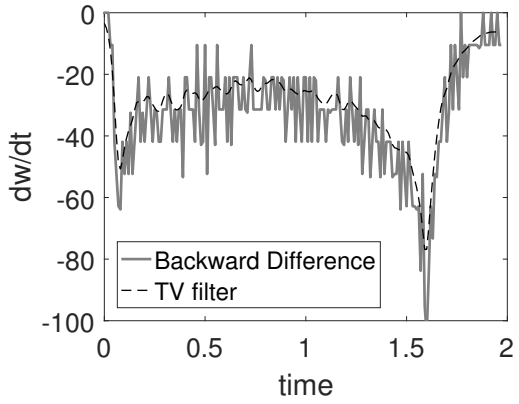

(b)

Figure 4.4: (a) IFW RPM data compared to the RPM resulting from Total Variation Minimization filter. (b) IFW $\frac{d\omega}{dt}$ data and the $\frac{d\omega}{dt}$ resulting from Total Variation Minimization filter.

Energy of the weld was calculated using Equation 4.2 using the TV minimized RPM. Torque was then calculated using Equation 4.6 and the weld energy was calculated. The plots of power, torque and weld energy can be seen in Figures 4.6 to 4.7.

4.3 Calculating Spindle Control

Matching weld power was designed to simulate the full-scale IFW by following a modified power curve of the IFW, accounting for the difference in specimen size. As stated previously the energy in the full-scale IFW (FS) is due to flywheel inertia and the initial rotational velocity of the flywheel.

$$E_{FS} = \frac{1}{2} I \omega^2 \tag{4.7}$$

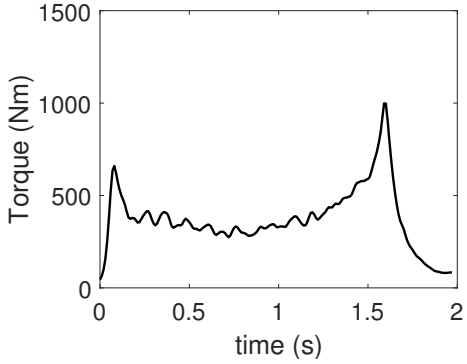

Figure 4.5: IFW torque versus time during the weld.

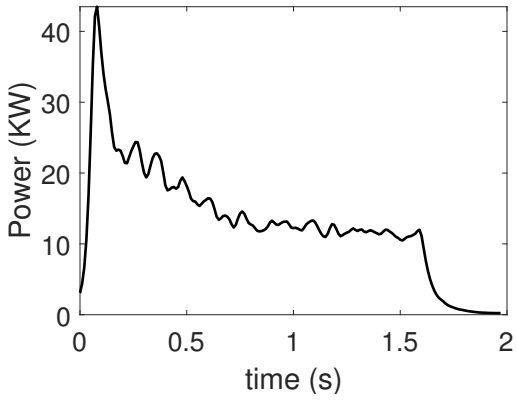

Figure 4.6: IFW power versus time during the weld.

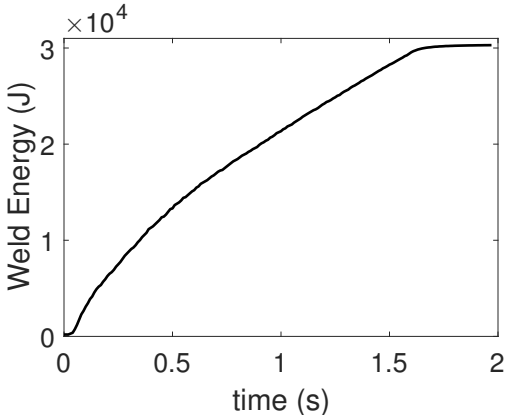

Figure 4.7: IFW weld energy versus time.

Taking the derivative of energy gives us the power ($\frac{dE}{dt}$) placed into the IFW.

$$\frac{d}{dt}E_{FS} = \frac{d}{dt}\frac{1}{2}I\omega_{FS}^2 \tag{4.8}$$

which leads to

$$\frac{dE_{FS}}{dt} = I\omega_{FS}\frac{d\omega_{FS}}{dt} \tag{4.9}$$

where ($\frac{d\omega_{FS}}{dt}$) is the deceleration of the flywheel. The power of the sub-scale SIFW (SS) is due to the torque of the spindle (τ_{SS}) and the speed of the spindle (ω_{SS}).

$$\frac{dE_{SS}}{dt} = \tau_{SS}\omega_{SS} \tag{4.10}$$

Setting the power of the sub-scale SIFW equal to the full-scale IFW gives us:

$$\frac{dE_{SS}}{dt} = \frac{dE_{FS}}{dt} \tag{4.11}$$

Rearranging the equations gives us a ω_{SS} as a function of the IFW flywheel inertia and rotational velocity data and the torque of the sub-scale SIFW as seen below:

$$\omega_{SS} = \frac{I\omega_{FS}\frac{d\omega_{FS}}{dt}}{\tau_{SS}} \tag{4.12}$$

This allowed inputs to control the RPM of the FSW spindle as a function of real time weld torque and the full-scale IFW RPM parameters.

4.4 Experiments

The ultimate expectation of these experiments is to determine an optimal method to simulate a full-scale IFW with a sub-scale specimen. Different experiments were run with different levels of force, power and RPM to determine the applicability of the factors and to determine the method that could be used to simulate a full-scale IFW with a sub-scale specimen. Table 4.2 shows the experiments run. The intermediate weld parameters consisting of torque, rpm and power are attempted to be minimized. While ultimately attempting to match the final weld results which con-

Table 4.2: The type of spindle control, power commanded, force commanded and the initial RPM of the experiments run to determine a method to simulate a FS IFW with a sub-scale specimen.

Experiment	**Spindle Control**	$\mathbf{P}_{CMD}/\mathbf{P}_{EXP}$	$\mathbf{F}_{CMD}/\mathbf{F}_{EXP}$	**Initial RPM**
1	Power	1	1	1500
2	Power	1	1	1000
3	Power	1	.565	1000
4	Power	1	.435	1000
5	Power	1	.387	1000
6	Power	2.4	1	1500
7	Power	3.5	1	1500
8	RPM	-	1	1500
9	RPM	-	.645	1500
10	RPM	-	.597	1500
11	RPM	-	.5	1500
12	RPM	-	.532	1250
13	RPM	-	.597	1000

sist of the final upset of the weld and the width of the HAZ. The ideal method will first minimize error between final results and secondarily minimize the error between intermediate results.

4.4.1 Calculating Accuracy of Results

The accuracy of the experiments are measured over time for some parameters and the ultimate result for others and compared to the expected values. The force, RPM, power, and torque of the welds are measured over time. The error was calculated from the expected value and the experimental value as seen in Equation 4.13.

$$Error = \frac{ExperimentalValue - ExpectedValue}{ExpectedValue} \tag{4.13}$$

The error is calculated at an interval of approximately every .02 seconds. The parameters measured over time have an average error determined. The final results for upset and the HAZ are looked at and an error is determined based on the end value using Equation 4.13. In addition to error, a ratio for the force, power, and rpm are taken. Equation 4.14 shows the calculation of this ratio.

$$Ratio_y = \frac{y_{experiment}}{y_{FS}} \tag{4.14}$$

A ratio equal to one, shown on the comparative figures, would show that the welding parameter matched the scaled value, whereas a ratio greater than one meant the experiment was greater than the scaled value.

4.5 Matching Spindle Power

Welds 2 through 7 were run while attempting to match weld power. Changes were made to power and force to change the weld results. Changes in the weld inputs are correlated to the outputs.

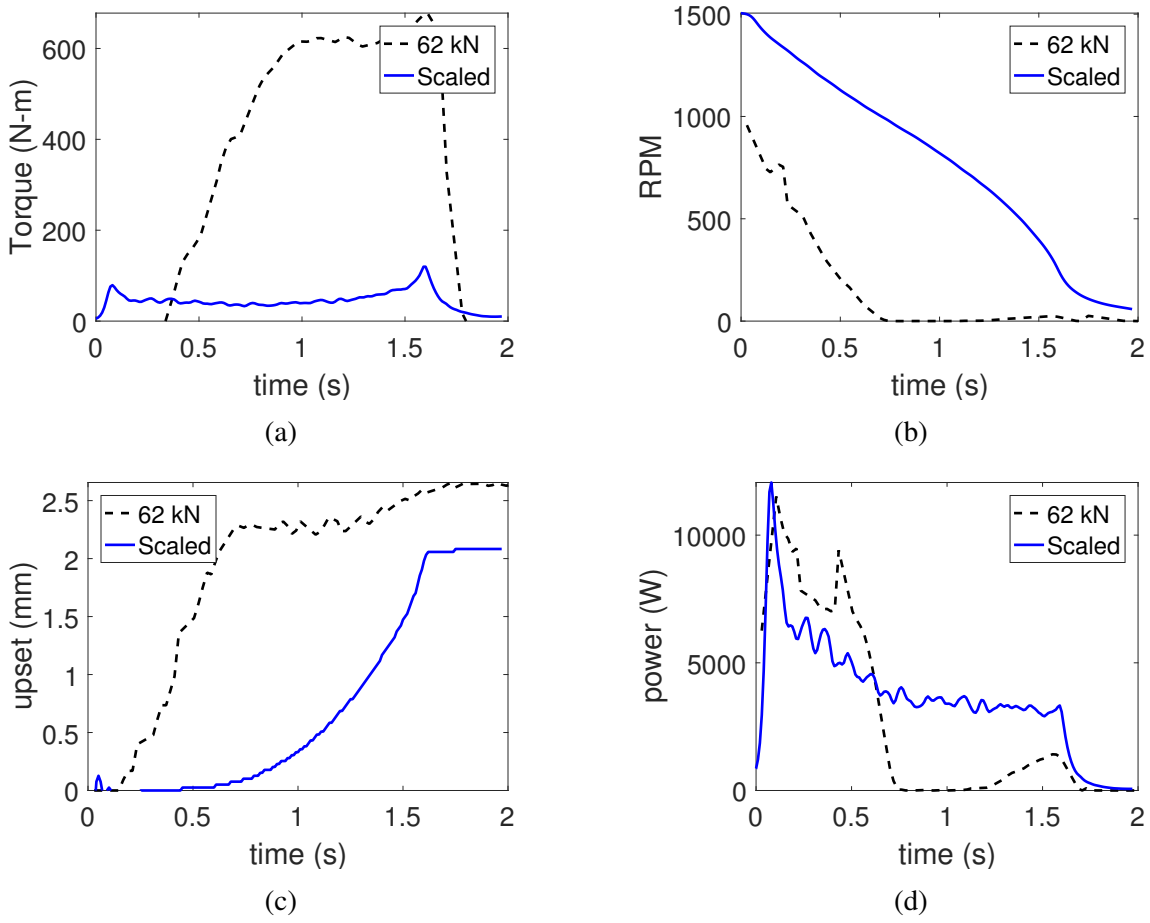

Figure 4.8: (a) Torque vs time data with expected power and force. (b) RPM vs time. (c) Upset vs time. (d) Power vs time.

4.5.1 Expected Power and Expected Force

A few problems existed while matching power at the expected force. The expected force created high torque values for a given the commanded RPM value. The torque values increased in the first 0.5 seconds as seen in Figure 4.8a. The increasing torque values drove the programmed RPM values down in Figure 4.8b, referring to Equation 4.12. A minimum RPM setting of 300 was set as a machine parameter to prevent spindle RPM going to zero. This allowed a torque limit of the spindle to be observed. At excessive torques, the spindle motor doesn't have enough power to rotate the spindle. In spite of the high levels of torque and the seizing of the spindle prevented energy from being placed into the weld after the first .6 seconds of the weld.

Expected forces and powers were altered to prevent the spindle from seizing while matching weld power. Reducing the force at the interface created the results in section 4.5.2. The alternate expected powers used were 3.5 times the expected and 2.4 times the expected and were run at welding forces of 80 kN and 62000 kN respectively and are seen in Sections 4.5.3.

4.5.2 Scaled Power with Changes in Commanded Force

Welds 3, 4, and 5 were run matching scaled weld power and changing the friction force of the weld to observe the affect the force had on the intermediate results of torque and final weld results of upset, energy density and the HAZ.

The magnitude of force used during the welding portion of the weld did cause noticeable effects on the intermediate outputs. Looking at the torque of the weld in Figure 4.9a shows that as force was decreased the torque at the interface decreased as well. The lower torques led both to a higher RPM and allowed the machine to run for the entirety of weld. As the force decreased from 27 kN to 24 kN the change in torque is less apparent, but on an average the 24 kN torque was closer to the expected value.

Looking at the final weld results of the HAZ combined with the upset and energy density can also help determine the force setting that would be preferred to use with matching weld power to simulate a full-scale IFW. As the force was decreased the upset went down with it. The decreasing in weld force let to an increase in energy density. Weld 4 showed the greatest resemblance to the FS IFW upset. However, weld 3 showed the greatest resemblance to the size of the HAZ.

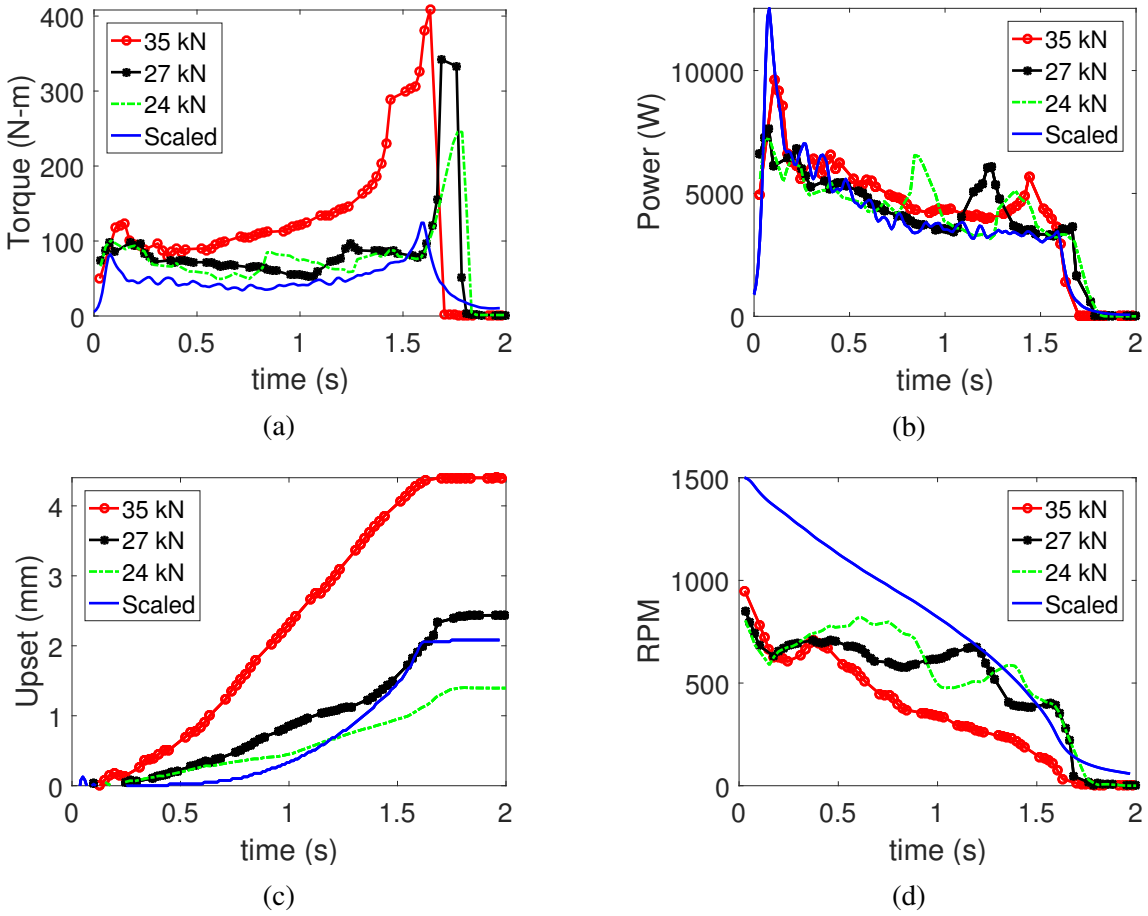

Figure 4.9: (a) Torque vs time with expected power at forces of 35, 27, and 24 kN. (b) Power vs time. (c) Upset vs time. (d) RPM vs time.

Figure 4.9c shows the final upset of the welds and Table B.1 in Appendix B shows the final width of the HAZ.

Each weld 3 4 and 5 identifies with a scaled output. Weld 3 resembled the scaled size of the HAZ but has the greatest error in torque, upset and RPM error. Weld 4 resembled the scaled upset, and has the same relative error as weld 5 when observing the RPM and torque error, but lacks the ability to match the width of the HAZ. Weld 5 had minimal error in the RPM and torque readings, but has maximum error in the HAZ and excessive error when looking at the upset. Taking all welds into consideration it would be recommended that while controlling the spindle a force between 35 kN and 27 kN be used. This would optimize the HAZ and the upset while minimizing the RPM and torque error.

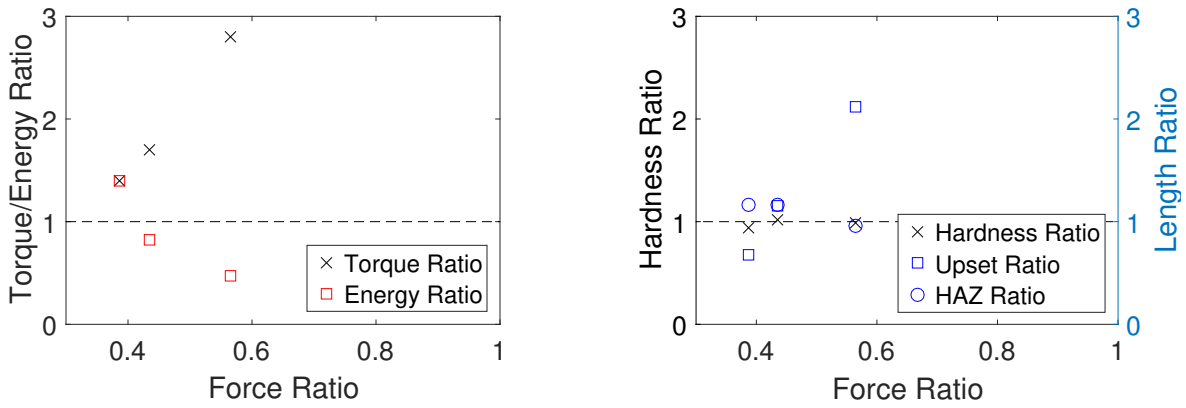

(a) (b)

Figure 4.10: (a) Torque ratio versus the force ratio. (b) Ratios of Hardness, upset, and HAZ versus the force ratio.

4.5.3 Increased Power Run

Weld 6 increased the power by a factor of 3.5 which allowed the weld to run the entirety of the weld. This factor made the RPM run at 1500 which was set as a machine limit for the SIFW runs. When the spindle RPM was at this value constantly, the weld torque dropped. The low torque value combined with the limitation of 1500 RPM of the machine prevented putting the amount of power desired into the weld. The final upset, and the RPM of this weld was significantly larger than the the expected values.

Weld 7 ran in matching weld power at 2.4 percent of the scaled power followed the RPM curve quite closely observed in Table B.1 in Appendix B and had minimal RPM error. The final upset, the torque values and power were not similar to the expected values. The welds with higher commanded power than expected gave higher final energies and greater upsets than what is expected from the IFW.

4.5.3.1 Conclusion of Matching Power

From this work we've learned that matching power can be accomplished with a good accuracy in power but little accuracy when compared to scaled values of RPM and torques of the weld. Reduction in the friction force leads to lower RPMs and higher torques. Reducing the friction force leads to reduced upset yet increases the size of the HAZ. These results leads to the conclusion that

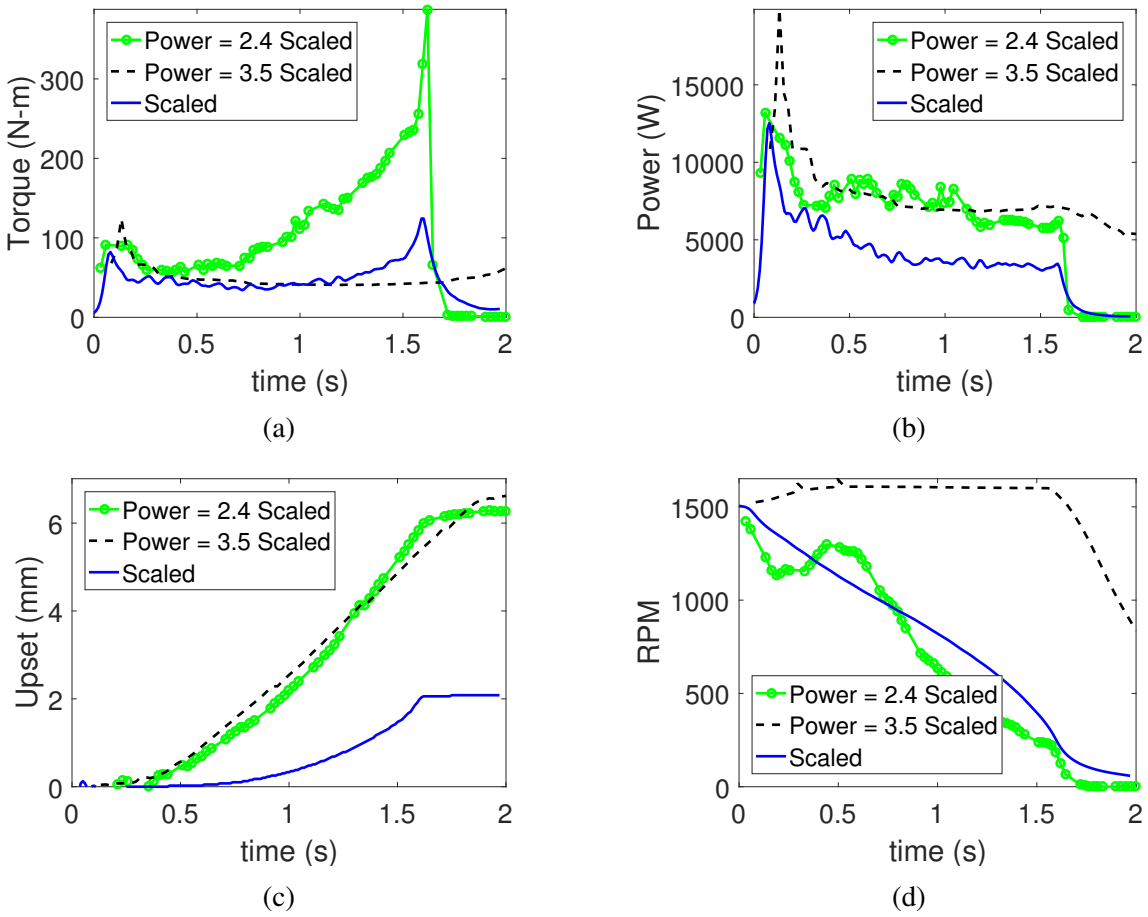

Figure 4.11: (a) Torque vs time data for 3.5 times the scaled power and 2.4 times the scaled power with 62 kN. (b) Power vs time. (c) Upset vs time. (d) RPM vs time.

when simulating a FS IFW while matching scaled power with a sub-scale specimen you must account for the reduction in area when considering the friction force to match other scaled outputs. However a decision must be made as to which parameter is the most important to match. For example a 35 kN force gave the prescribed width of HAZ but the force of 27 kN gave a more similar torque, energy density, minimum hardness and upset that more closely matched the FS IFW.

4.6 Controlling Spindle RPM

Welds 8 through 13 were run matching weld RPM. Changes were made to initial RPM and force to change the weld results. Changes in the weld inputs are correlated to the outputs.

4.6.1 Following the RPM curve

Welds 8 through 11 were run with the scaled RPM while changing the applied force. The spindle controlled the RPM of the welds as seen in Figure 4.12a repeatedly with negligible deviation with changes in force.

Decreasing the force while controlling the spindle in RPM mode caused noticeable trends in the results. The inputs for spindle control are RPM and force while the the final weld results consist of upset, energy density and the width of the HAZ. Increasing the force increased the upset as shown in Figure 4.13a. It is noticed that the weld that was run with 36 kN of force related closest to the expected upset and had a good energy density ratio. The width of the HAZ and the energy density were both inversely related to the force of the weld as seen in Figure 4.13a, exact values

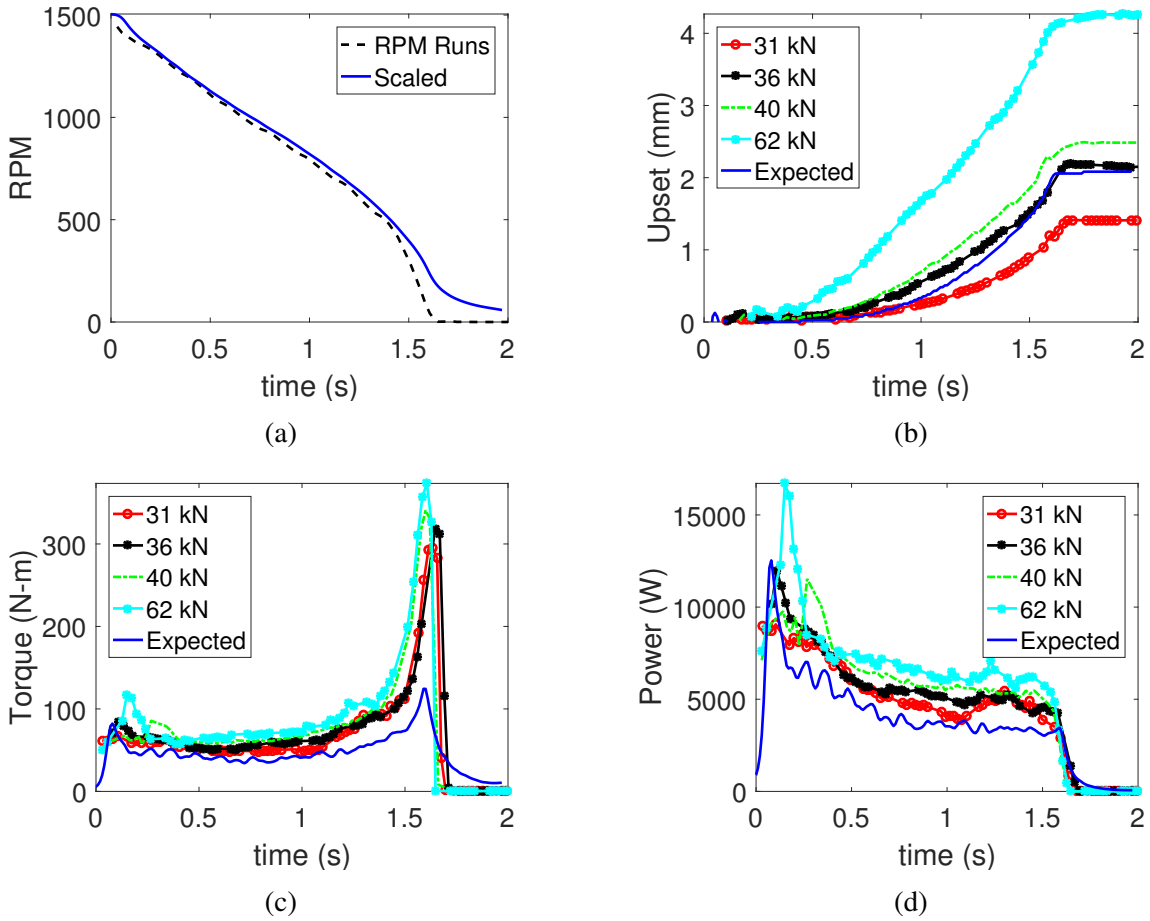

Figure 4.12: (a) RPM vs time for the RPM controlled welds with forces of 31, 36, 40, 62 kN. (b) Upset vs time. (c) Torque vs time. (d) Power vs time.

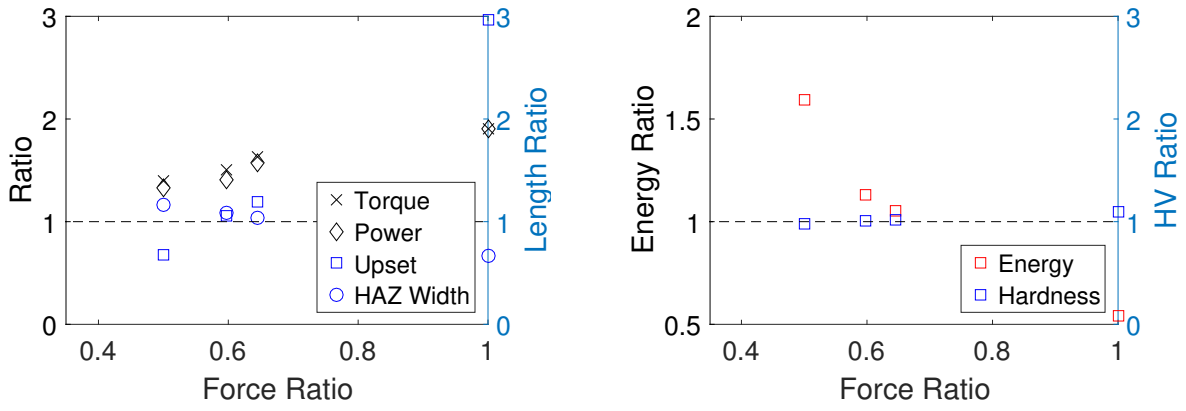

(a) (b)

Figure 4.13: (a) Force ratio versus the ratios of torque, power upset and HAZ width for the weld experiments matching weld RPM with changes in force. (b) Force ratio versus the ratios of hardness and energy for the weld experiments matching weld RPM with changes in force.

can be seen in Table B.2 in Appendix B. As the force was increased the width of the HAZ went down. The expected width of the HAZ is 2.4 mm while the optimal force that would create a HAZ width of that size would be greater that the 40 kN weld while matching weld RPM.

Decreasing the force of the weld also decreased the torque and power of the weld as can be seen in Figure 4.13a. The ratio of the torque and power went down as the commanded force was decreased. Figure 4.13a show that as force was reduced the torque and power got closer to the expected values. However an optimal force was not found that actually produced the expected power and torque values. If minimizing the error in power and torque was the preferred method, a weld with a force less than 31 kN would be suggested.

4.6.2 Reduced RPM Runs with Reduced Force

Welds 12 and 13 were run with a fraction of the scaled RPM to determine the effect the RPM would have with a reduced force of 35 kN on the HAZ, upset and final energies of the weld. Decreasing the RPM to a value of 5/6 of the scaled RPM produced a weld with an upset of 1.76 mm with a force of 32000 newtons. The run that initialized at 1000 RPM and was 2/3 of the scale value gave an upset of 1.98 mm only a slight percentage off of the FS IFW. The HAZ sizes went down as the RPM was decreased.

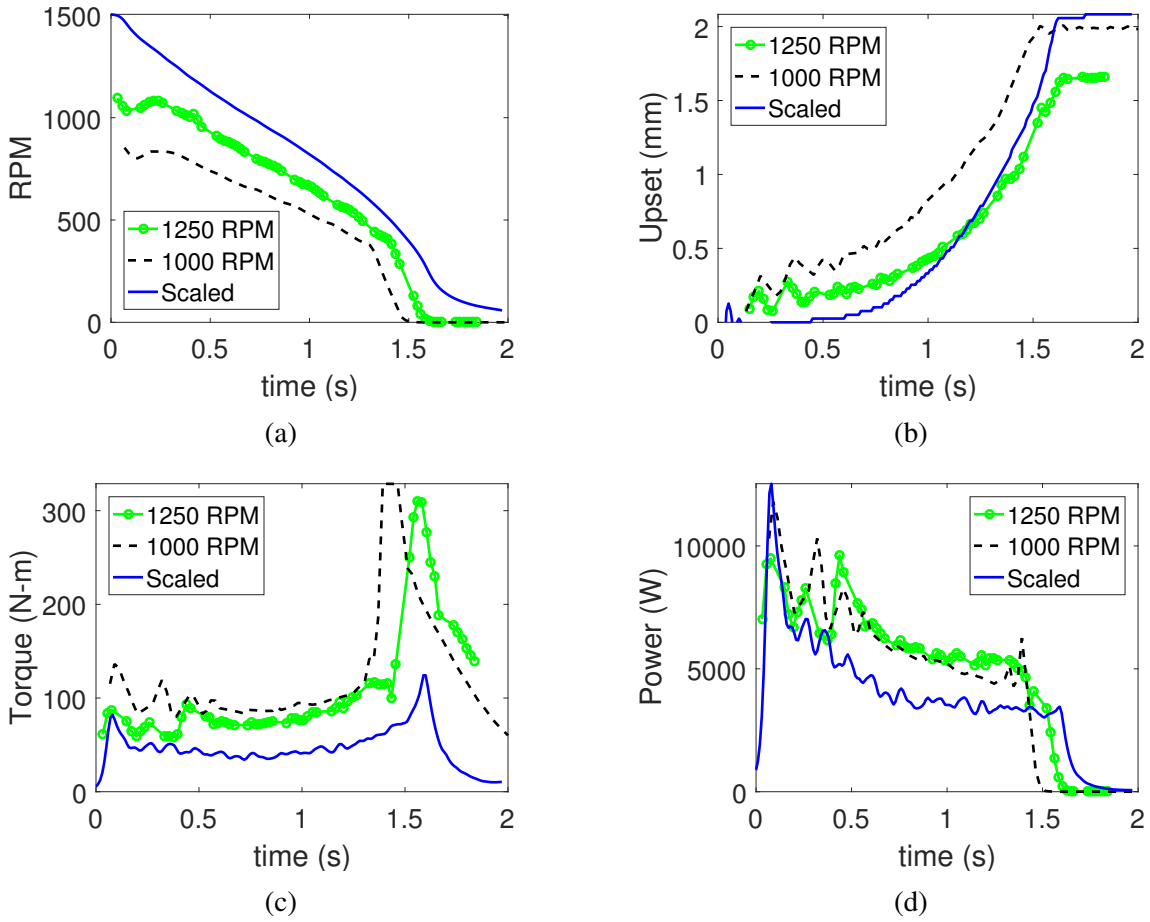

Figure 4.14: (a) RPM vs time for the RPM controlled welds at 1250 and 1000 RPM. (b) Upset vs time. (c) Torque vs time. (d) Power vs time.

Torque is noticeably affected by the RPM, as seen in Figure 4.15, while the power of the weld seemed relatively constant. Despite the changes in RPM, the average power at a given time was nearly equal. However, increasing the RPM did reduce the torque of the weld.

4.6.2.1 Matching RPM Conclusion

From matching the RPM while changing the force we have learned that the higher forces still give similar trends with HAZ, energy density, upset and torque values. The force that gave a similar HAZ, energy density, and upset was 40 kN and this produced great results. A higher initial RPM led to lower torques when compared to similar forces of the power match runs but the upset and the HAZ were smaller. The RPM runs would be preferred based upon results for all outputs,

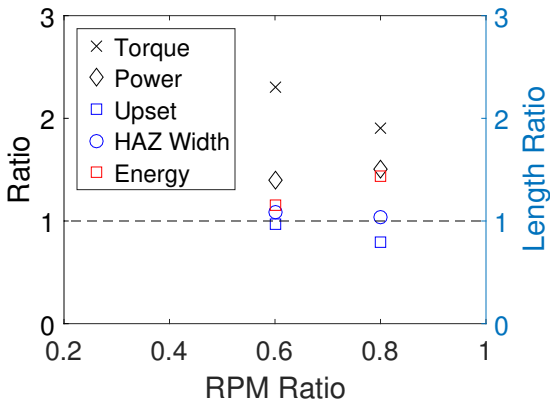

Figure 4.15: RPM ratio versus the torque, power, upset and the HAZ width ratios for the weld experiments varying the scaled RPM.

with the exception of power and torque. This means that to simulate a FS IFW with a sub-scale specimen the preferred method when matching RPM would have a force that gave respectable upsets and HAZ width which could be concluded from these welds that a force between 35 kN and 40 kN could be used.

4.7 Conclusion

Two methods of spindle control provide similar results when accounting for the torque. The torque of the weld was closely matched to the scaled value for the power controlled welds, while the torque for the RPM controlled welds was higher than the scaled value. The higher friction forces produced higher torques of the RPM and power match welds. It can be concluded that the torque factor is not as theorized and the FS and SS IFW and torque does not scale as described. A torque factor cannot be concluded from this paper as it appears to be a function of the force used.

The force of the weld could be modified for both methods of spindle control to optimize the size of the HAZ, upset, and the minimum hardness of the weld. As seen while matching power, the optimum force to use would be around 35 kN. While matching weld rpm, an optimum force lies between 35 kN and 40 kN which would produce weld results that correlated with the expected HAZ width, energy density, hardness and weld upset.

Power control provided great results when considering the HAZ, upset, torque, power and energy density. The power control when set at 27 kN provided results that were near to the expected scaled values in every area with the exception of torque, but towre was within a ration of 1.7.

CHAPTER 5. CONCLUSION

A modified FSW can simulate a full scale IFW with a sub scale specimen with certain machine modifications and accounting for parameter adjustments based upon specimen size. The FSW machine changes consisted of obtaining precise measurements for weld torque and position. It also included changes to the force control parameters to enable accurate force control. A sub-scale specimen weld can simulate full-scale welded specimen with the emphasis of matching the HAZ and upset.

Whether matching RPM or the power of the weld the force can be modified to produce sub-scale weld that simulated a full-scale weld, giving similar weld HAZ width, hardness and upset. The following is a list of parameters and their theoretically scaled and actual scaled values while controlling the spindle and matching power or RPM.

- The force of the weld while in power (RPM) mode should be given an approximate force of 27 (35) kN. This provides an actual scaled factor of 0.123 (0.159) compared to the theoretical scaled value of 0.282
- The resultant torque at the forces above on average would be 0.213 (0.204) when compared to the theoretical scaled value of 0.125
- The energy density ratios at these forces would be a scaled value of .82 (1.05) when compared to a theoretical value of 1.
- While running in power mode at the above force, the RPM will be on average 70 percent lower than the expected value.
- While running in RPM mode at the above force, the power error on average will be 160 percent higher than the expected value.

REFERENCES

[1] L.D' ALvise, E. Massoni, S.J. Walloe, Finite element modelling of the inertia friction welding process between dissimilar materials, *Journal of Materials Processing Technology*, 125-126 1, 2, 6

[2] Fundamentals of Friction Welding, *Welding Fundamentals and Processes* Vol 6A, ASM Handbook ASM International, 2011 p 179-185 1, 3, 6

[3] Friction Welding - Critical assessment of literature, *Science and Technology of Welding and Joining*, 12:8, 738-759 1, 2

[4] V.I. Vill, *Friction Welding of Metals*, translated from the Russian, American Welding Society, 1962 1

[5] Wenya Li, Achilles Vairis, Michael Preuss & Tiejun Ma (2-16): *Linear and rotary friction welding review*, International Materials Review 1

[6] M. Kimura, K. Suzuki, M. Kusaka, K. Kaizu, *Effect of friction welding condition on joining phenomena, tensile strength, and bend ductility of friction welded joint between pure aluminum and AISI 304 stainless steel* Journal of Manufacturing Processes, January 2017, p 116-125 1

[7] D.E. Spindler, Welding Journal, March 1994, p 37-43 2

[8] R.G. Ellis, *Welding Journal 51* (1972) 183-197 2

[9] Z.W. Huang, H.Y. Li, M. Preuss, M. Karadge, P. Bowen, S. Bray, and G. Baxter, Inertia Friction Welding Dissimilar Nickel-Based Superalloys Alloy 720Li to IN718 *Metallurgical and Materials Transactions A* Volume 38A, July 2007–1609 2, 3

[10] F. Daus, H.Y. Li, G. Baxter, S. Bray & P. Bowen (2007, Mechanical and microstructural assessments of RR1000 and IN718 inertia weld - effects of welding parameters, *Materials Science and Technology*, 23:12, 1424-1432

[11] Haka Ates, Mehmet Turker, Adem Kurt, Effect of friction pressure on the properties of friction welded MA956 iron-based superalloy *Materials & Design* 28(2007) 948-953

[12] F.F. Wang, W.Y. Li, J.L. Li, A. Vairis Process parameter analysis of inertia friction welding nickel-based superalloy *Int. Journal Advanced Manufacturing Technology* (2014) 71:1909-1918

[13] http://www.weldcor.ca/encyclopedia.html, 2017 vii, 1, 2, 3

[14] L. Rudin, S. Osher, and E. Fatemi. Nonlinear total variation based noise removal algorithms. *Physica D*, 60:259268, 1992. 21

[15] Ahmet Can, Mumin Sahin, Mahmut Kucuk. Modelling of Friction Welding. *Unitech Gabrovo*, November 2010 7

APPENDIX A. DRAWINGS

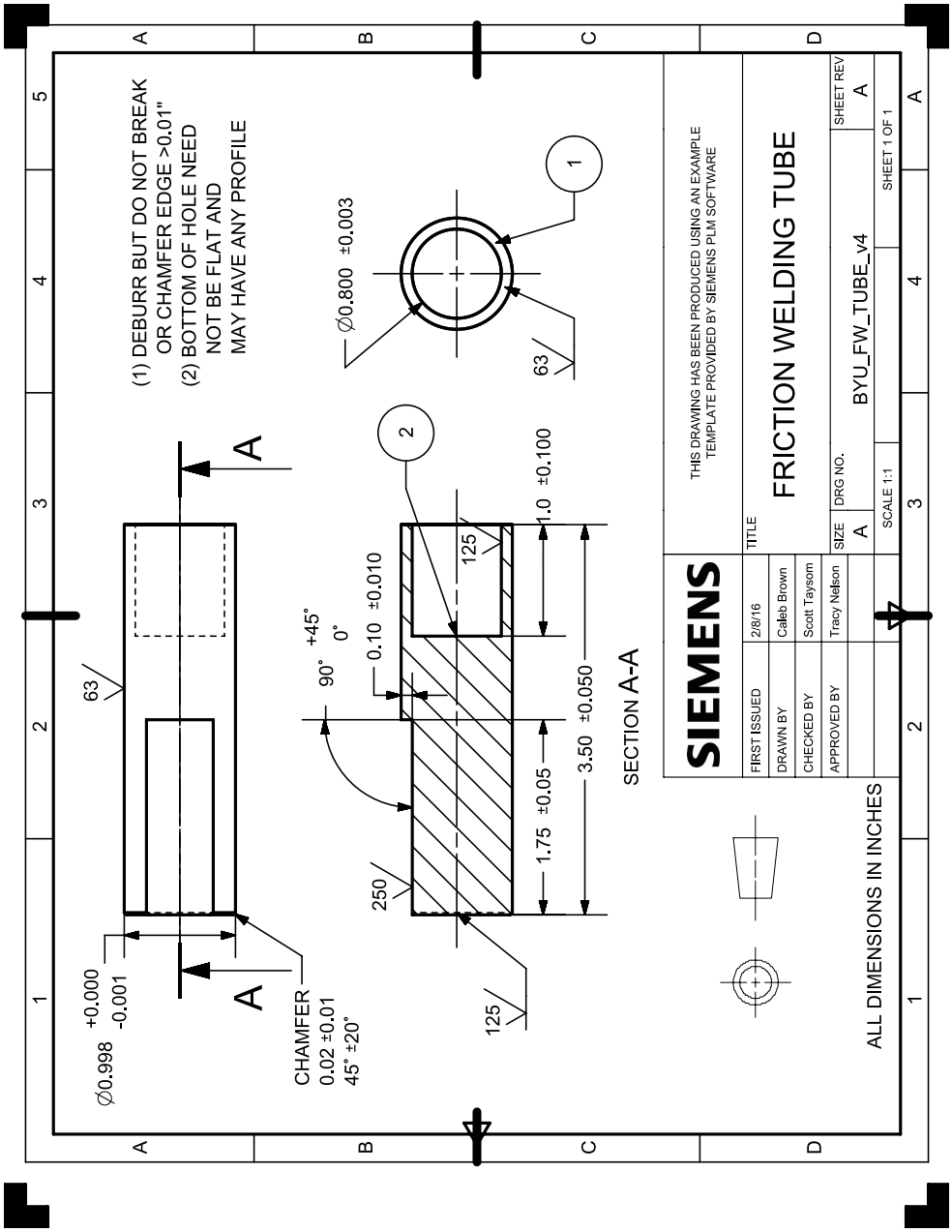

Figure A.1: BYU specimen sample geometry.

ITEM NO.	PART NUMBER	DESCRIPTION	QTY.
1	Lower Fixture Plate		1
2	RU 178a Bearing		1
3	Upper Fixture		1
4	ER-40 Collet		1
5	Load Cell Mounting Plate		2
6	Load Cell Mount		2
7	Load Cell		1
8	Torque Meter Lever Arm		1

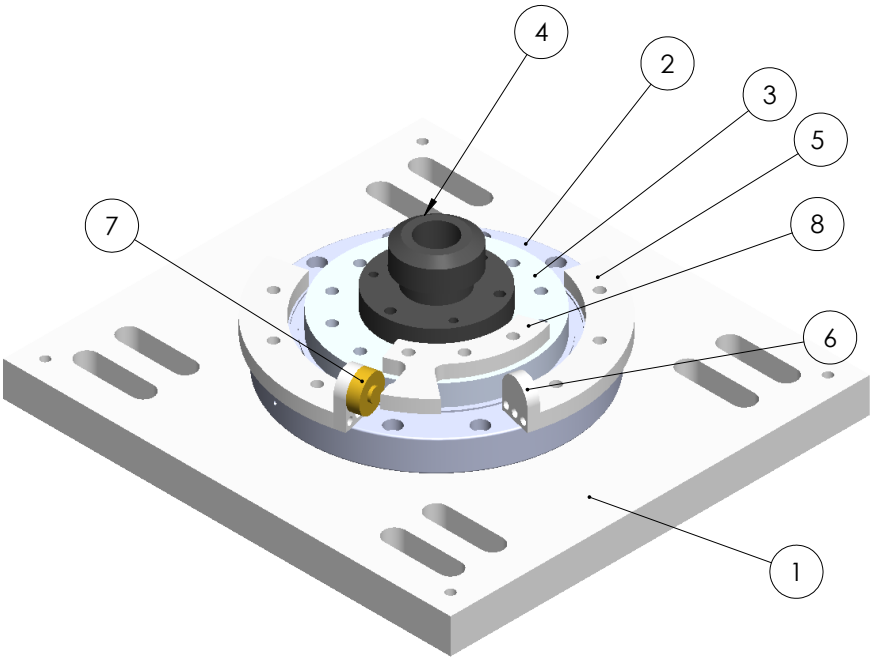

UNLESS OTHERWISE SPECIFIED:
DIMENSIONS ARE IN MILLIMETERS
SURFACE FINISH:
TOLERANCES:
LINEAR:
ANGULAR:

FINISH:

DEBURR AND BREAK SHARP EDGES

DO NOT SCALE DRAWING

REVISION

	NAME	SIGNATURE	DATE
DRAWN			
CHK'D			
APPV'D			
MFG			
Q.A			

TITLE:

MATERIAL:

DWG NO. torquemeter2

A4

WEIGHT:

SCALE:1:10

SHEET 1 OF 1

Figure A.2: BYU Torque Meter.

APPENDIX B. TABLES FOR RESULTS

Table B.1: Inputs and resultant outputs, average and final errors of power controlled welds.

Inputs			**Outputs**					
Run	P_{CMD}/P_{EXP}	F_{CMD}/F_{EXP}	RPM Error (%)	Torque Error (%)	Upset Error (%)	HAZ (mm)	Minimum Hardness (HV)	Energy Density Error (%)
-	FS IFW	FS IFW	-	-	-	2.4	319.1	-
2	1	1	85.3	877.7	27.5	1.6	360.0	-50
3	1	.565	54.6	179.8	111.4	2.3	315.2	-52
4	1	.435	31.6	66.3	17.1	2.8	323.3	-18
5	1	.387	29.4	60.7	-32.7	2.8	296.5	39
6	3.5	1	82.7	34.5	344	2.7	316.9	-38
7	2.4	1	20.3	135.1	202	1.8	380.0	-51

Table B.2: Inputs and resultant outputs, average and final errors of RPM controlled welds.

Inputs			**Outputs**					
Run	P_{CMD}/P_{EXP}	F_{CMD}/F_{EXP}	Power Error (%)	Torque Error (%)	Upset Error (%)	HAZ (mm)	Minimum Hardness (HV)	Energy Density Error (%)
-	FS IFW	FS IFW	-	-	-	2.4	319.1	-
8	1	1	76.4	93.0	104.9	1.6	349.5	-46
9	1	.645	58.0	63.7	19.7	2.5	324.4	5
10	1	.597	41.6	47.3	5.1	2.6	320.9	13
11	1	.5	34.7	40.5	32.2	2.8	312.0	59
12	.833	.532	50.9	87.8	20.4	2.6	316.5	15
13	.597	47.9	143.9	1.98	4.8	2.5	324.5	44

APPENDIX C. FORCE CONTROL TESTING MECHANISM

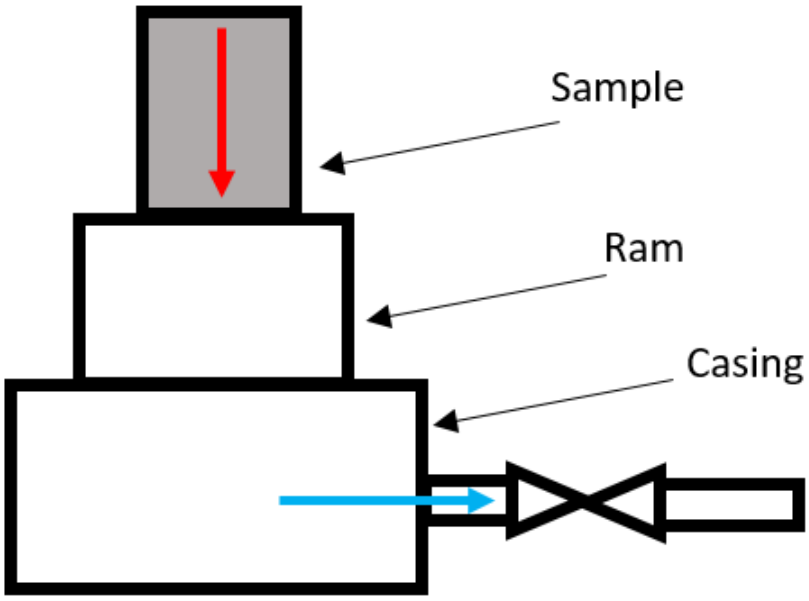

Figure C.1: Force Control testing mechanism